



# Mixing state of individual submicron carbon-containing particles during spring and fall seasons in urban Guangzhou, China: a case study

G. Zhang<sup>1,2</sup>, X. Bi<sup>1</sup>, L. Li<sup>3</sup>, L. Y. Chan<sup>1</sup>, M. Li<sup>3</sup>, X. Wang<sup>1</sup>, G. Sheng<sup>1</sup>, J. Fu<sup>1,3</sup>, and Z. Zhou<sup>3</sup>

<sup>1</sup>State Key Laboratory of Organic Geochemistry, Guangzhou Institute of Geochemistry, Chinese Academy of Sciences, Guangzhou 510640, China

<sup>2</sup>Graduate University of Chinese Academy of Sciences, Beijing 100049, China

<sup>3</sup>School of Environmental and Chemical Engineering, Shanghai University, Shanghai 200444, China

Correspondence to: X. Bi (bixh@gig.ac.cn)

Received: 30 October 2012 – Published in Atmos. Chem. Phys. Discuss.: 19 December 2012

Revised: 26 March 2013 – Accepted: 12 April 2013 – Published: 7 May 2013

**Abstract.** Growing evidence suggests that the size-resolved mixing state of carbon-containing particles is very critical in determining their optical properties, atmospheric lifetime, and impact on the environment. However, still little is known about the mixing state of particles in the urban area of the Pearl River Delta (PRD) region, China. To investigate the mixing state of submicron carbon-containing particles, measurements were carried out during spring and fall periods of 2010 using a single-particle aerosol mass spectrometer (SPAMS). Approximately 700 000 particles for each period were detected. This is the first report on the size-resolved mixing state of carbon-containing particles by direct observations in the PRD region. Cluster analysis of single-particle mass spectra was applied to identify carbon-containing particle classes. These classes represented ~80 % and ~90 % of all the detected particles for spring and fall periods, respectively. Carbon-containing particle classes mainly consisted of biomass/biofuel burning particles (Biomass), organic carbon (OC), fresh elemental carbon (EC-fresh), internally mixed OC and EC (ECOC), internally mixed EC with sulfate (EC-Sulfate), vanadium-containing ECOC (V-ECOC), and amines-containing particles (Amine). In spring, the top three ranked carbon-containing particle classes were ECOC (26.1 %), Biomass (23.6 %) and OC (10 %), respectively. However, the fraction of Biomass particles increased remarkably and predominated (61.0 %), while the fraction of ECOC (3.0 %) and V-ECOC (0.1 %) significantly decreased in fall. To highlight the influence of monsoon on the prop-

erties of carbon-containing particles in urban Guangzhou, their size distributions, mixing state, and aerosol acidity were compared between spring and fall seasons. In addition, a case study was also performed to investigate how the formation of fog and haze influenced the mixing state of carbon-containing particles. These results could improve our understanding of the mixing state of carbon-containing particles, and may also be helpful in modeling the climate forcing of aerosol in the PRD region.

## 1 Introduction

Carbonaceous aerosols strongly affect the visibility and energy balance of Earth by either scattering or absorbing solar radiation (Jacobson, 2001; Ramanathan and Carmichael, 2008). Acting as cloud condensation nuclei (CCN) (Sun and Ariya, 2006; Jacobson, 2006), they also contribute to an indirect effect on global climate. Depending on particle size and chemical composition, they may also cause severe health problems (Pöschl, 2005; Turpin and Huntzicker, 1995). Carbonaceous aerosols are normally divided into two major fractions: organic carbon (OC) and elemental carbon (EC). OC could be directly emitted into the atmosphere from both anthropogenic and natural sources, and also formed via conversion of volatile precursors (Chung and Seinfeld, 2002; Jacobson et al., 2000). Activation capability of OC might be comparable to that of sulfate (Sun and Ariya, 2006), as a

function of mixing state (Svenningsson et al., 2006). Generated in a variety of combustion processes (Bond et al., 2013), EC typically represents a relatively low fraction compared to OC in the atmosphere (Clarke et al., 2004; Yu et al., 2010). However, it is a primary light absorption constituent and significantly contributes to positive radiative forcing (Jacobson, 2001).

Some measurement campaigns, such as PRIDE-PRD (Program of Regional Integrated Experiments of Air Quality over Pearl River Delta), have been carried out in the Pearl River Delta (PRD) region, China (e.g., Xiao et al., 2011; Zhang et al., 2008). These studies showed that carbonaceous aerosols represent a major fraction of submicron aerosol particles (Chan and Yao, 2008; Andreae et al., 2008), and the attenuation of light caused by carbonaceous aerosols is extremely important in the PRD region (Cheng et al., 2008; Yu et al., 2010). Knowledge on mixing state of carbon-containing particles is a necessary prerequisite to accurately determine their contribution to the visibility degradation, as well as to help gain an understanding on their roles in the regional climate. Evidence also implies that aerosol mixing state plays a critical role in controlling concentrations of CCN in polluted urban areas (Cubison et al., 2008). Furthermore, model prediction of number concentration of CCN is highly sensitive to the assumed size-resolved mixing state (Stroud et al., 2007). Mixing state of individual particles is available from single-particle measurements, allowing insights into sources, atmospheric processing, optical and cloud properties of atmospheric aerosols (Prather, 2009; Pratt and Prather, 2012). Results from worldwide measurements showed large variabilities in the mixing state of carbonaceous aerosols, resulted from various factors (e.g., local sources, atmospheric ageing and long-range transport). Dall'Osto and Harrison (2012) linked OC-containing particle classes to various sources, through comparison of OC-containing particle classes with factors resolved by positive matrix factorization from a data set obtained by an aerosol mass spectrometer. Healy et al. (2012) revealed the influence of the sources and long-range transport on the size-resolved mixing state of EC-containing particles in Paris. Moffet and Prather (2009) observed a rapid coating process of OC and sulfate on EC cores in the polluted atmosphere of Mexico City, which would substantially enhance the absorption capacity of EC. Qin et al. (2012) reported that carbonaceous particles dominantly mixed with sulfate in the summer, while in the fall mainly with nitrate, in California, due to favorable condensation of ammonium nitrate. Over two major aircraft campaigns in California, Cahill et al. (2012) showed that carbonaceous particles such as biomass burning, aged soot, and OC classes represented a major fraction of all the observed particles; and that the majority of carbonaceous particles were internally mixed, varied temporarily, and were highly influenced by secondary species. The authors further suggested that temporal variations of aerosol physical and chemical properties, depending on their mix-

ing state, should be considered in predictions of their climate impacts. However, direct observations on the size-resolved mixing state of carbon-containing aerosol in the PRD region or in other parts of China were limited. Yang et al. (2012) investigated the influence of the meteorological condition on the mixing state of carbonaceous particles in Shanghai and showed dramatic addition of secondary species onto fresh EC or biomass-burning particles under hazy conditions. Similarly, Fu et al. (2012) observed four types of carbonaceous aerosols in the Shanghai atmosphere, and found that most of the particles were coated with secondary organic aerosols. Based on transmission electron microscopy, Li et al. (2011b) also found more fractions of internally mixed EC particles in the polluted air of northern China. Single-particle soot photometer measurements revealed that the number fraction of internally mixed EC was highly variable and could be as high as  $\sim 70\%$  in the PRD region, while the detailed information on mixing state is limited by this instrument (Huang et al., 2011, 2012).

Situated in the PRD region, the atmospheric condition of Guangzhou is under a strong influence of the Asian monsoon system. Southwesterly to southeasterly monsoon brings relatively clean air from the sea in summer and spring, and northeasterly wind carries relatively polluted air masses across northern cities in fall and winter. The inherent seasonality in monsoon circulation results in dryness during fall and winter seasons, and wetness during spring and summer seasons. Herein, we applied real-time single-particle aerosol mass spectrometer (SPAMS) measurements to reveal the major single-particle classes of carbon-containing particles, and to explore the seasonal variability of their number fraction as a function of vacuum aerodynamic diameter ( $d_{va}$ ), aerosol mixing state with secondary species, and particle acidity in the spring and fall of 2010 as a case study, in the urban area of the PRD region. Differences in meteorological conditions leading to the variations in aerosol mixing states are also discussed.

## 2 Experiment setup and data analysis

### 2.1 Meteorological conditions during the sampling

Single-particle measurements were carried out nearly continuously at the Guangzhou Institute of Geochemistry (GIG), Chinese Academy of Sciences, during late spring (between 30 April and 22 May 2010), and fall (between 5–20 November 2010), using a SPAMS (Li et al., 2011a) developed by Hexin Analytical Instrument Co., Ltd. (Guangzhou, China). The measurement site was described elsewhere (Bi et al., 2011). The ambient temperature during sampling in spring varied between 19–33 °C, with an average of 26 °C; and average relative humidity (RH) was 81 %, ranging between 22–100 %. The ambient temperature during the fall period was in the range of 16–38 °C, with an average of

23 °C; and average RH was 54 % with 21 % the lowest and 82 % the highest. Twenty four hour air mass back-trajectory for each day (ending at 00:00 LT, local time) during both spring and fall was calculated by the HYSPLIT 4.9 (HYbrid Single-Particle Lagrangian Integrated Trajectory version 4.9) transport model (<http://ready.arl.noaa.gov/HYSPLIT.php>) (Draxler and Rolph, 2012). Based on the model, air masses from southeastern and southwestern marine regions dominated throughout the spring, while during the fall air masses from northeastern continental areas were prevalent, as shown in Fig. 1.

## 2.2 Methodology of single-particle detection and data analysis

The particle detection method of SPAMS was described by Li et al. (2011a). Briefly, aerosol particles are introduced into SPAMS through a critical orifice, then focused and accelerated to specific velocities, which are determined by their flight time through two continuous diode Nd:YAG (neodymium: yttrium aluminum garnet) laser beams (532 nm) in the sizing region. The particles are subsequently desorbed/ionized by a pulsed laser (266 nm) triggered exactly based on the velocity of the specific particle. The positive and negative fragments generated are recorded with  $d_{va}$ .

In this study, approximately 700 000 particles for each period, with  $d_{va}$  ranging between 0.2 and 1.2  $\mu\text{m}$ , were chemically analyzed with both positive and negative ion spectra. This amount of data should be sufficient to perform a statistical analysis, and thus to provide representative results in this study. Particle size and mass spectra information were used to create the peak lists with a minimum area threshold of 20 arbitrary units (background noise was generally lower than 5 units) by using TSI MS-Analyze software. The peak lists were then imported into MATLAB (The Mathworks Inc.) and analyzed with YAADA 2.1 (Yet Another ATOFMS Data Analyzer; [www.yaada.org](http://www.yaada.org)). Peak identification described in this paper corresponded to the most probable assignments for each particular mass to charge ratio ( $m/z$ ). An adaptive resonance theory based neural network algorithm (ART-2a) was applied to cluster individual particles into separate groups based on the presence and intensity of ion peaks in individual single-particle mass spectra (Song et al., 1999) with a vigilance factor of 0.75, learning rate of 0.05, and 20 iterations. At first 250 clusters in spring and 200 clusters in fall dominated the initially generated clusters, representing more than 90 % of all the analyzed particles, and were manually merged to produce 11 and 10 final particle classes based on the spectral similarities, respectively.

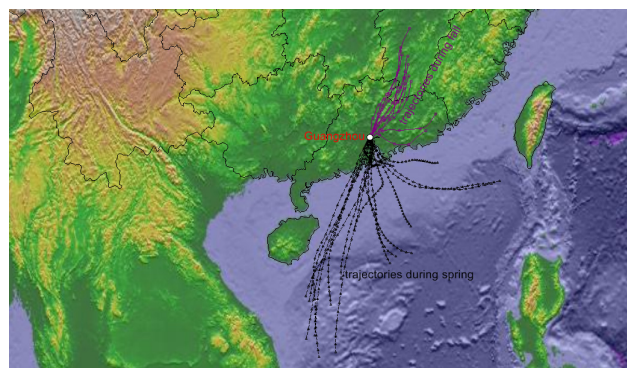


**Fig. 1.** Daily backward air-mass trajectories reaching the urban Guangzhou site ending at 500 m a.s.l. and 00:00 LT during spring (black lines) and fall (purple lines) sampling periods.

## 2.3 Scanning mobility particle sizer with a condensation particle counter (SMPS + C)

Particle size distribution measurements were performed using a cylindrical scanning differential mobility analyzer upstream of a condensation particle counter (SMPS + C 5.401; GRIMM Aerosol Technik GmbH & Co. KG) during 7–21 May 2010 (Zhang et al., 2012). Size distribution readings from SMPS + C in the discussion section of this paper only included the particles with  $d_m$  (mobility diameter) lower than 521 nm. Particle number concentration obtained from the collocated SMPS + C was commonly utilized to scale the particle number counts from SPAMS, in order to obtain an approximately quantitative view (e.g., Reinard et al., 2007; Bein et al., 2006; Healy et al., 2012), although it might introduce an error in scaled number counts for different particle classes (Gross et al., 2006). The size-dependent hourly scaling factors are shown in Fig. S1 from the Supplement. It is noted that the collocated SMPS + C was only operated for approximately 174 h while SPAMS ran 376 h during the spring sampling period. Thus the quantitative results mentioned in the following only referred to the period when the collocated SMPS + C was running.

## 3 Results and discussion

The chemical patterns of the analyzed particles were determined through the classification of particles into the distinct catalogues. As listed in Table 1, 7 out of 11 and 6 out of 10 single-particle classes during spring and fall periods, respectively, were assigned as carbon-containing particles, referring to particle classes containing OC, EC, or their combinations (Liu et al., 2003; Bahadur et al., 2010). Carbon-containing particles consisted of particle classes corresponding to biomass/biofuel burning particles (Biomass), OC-dominant particles lacking or with negligible EC signals (OC), internally mixed OC and EC (ECOC), fresh EC

particles (EC-fresh), EC-dominant particles mainly mixed with sulfate (EC-Sulfate), and vanadium-containing ECOC (V-ECOC). In addition, there was an amine-containing particle class (Amine), which was unique to the spring period. Carbon-containing particle classes described here generally resembled those observed by Moffet et al. (2008) in Mexico City. Other single-particle classes, such as dust and sea salt, were grouped together with unclassified particles as “Others”.

Overall, the average digitized mass spectrum of carbon-containing particles in Fig. 2 shows that  $39[\text{K}]^+$ , dual polarity EC cluster ions ( $12[\text{C}^{+/-}]$ ,  $24[\text{C}_2^{+/-}]$ ,  $36[\text{C}_3^{+/-}]$ , ...,  $[\text{C}_n]^{+/-}$ ), as well as fragments from secondary inorganic species of sulfate ( $-97[\text{HSO}_4]^-$ ), nitrate ( $-46[\text{NO}_2]^-$  and  $-62[\text{NO}_3]^-$ ), and ammonium ( $18[\text{NH}_4]^+$ ) were the dominant peaks. The peak at  $m/z$  39 may also be assigned to an organic fragment  $39[\text{C}_3\text{H}_3]^+$  (Silva and Prather, 2000), when organics dominate in particles. Most carbon-containing particles were internally mixed with sulfate ( $\sim 80\%$  in number) and/or nitrate ( $\sim 60\%$ ), indicating some degree of atmospheric ageing (Toner et al., 2008). Other dominant peaks at  $m/z$   $15[\text{CH}_3]^+$ ,  $27[\text{C}_2\text{H}_3]^+$ ,  $29[\text{C}_2\text{H}_5]^+$ ,  $37[\text{C}_3\text{H}]^+$ ,  $43[\text{C}_2\text{H}_3\text{O}]^+$ ,  $51[\text{C}_4\text{H}_3]^+$ ,  $55[\text{C}_4\text{H}_7]^+$ ,  $57[\text{C}_4\text{H}_9]^+$  and  $63[\text{C}_5\text{H}_3]^+$  were typically characteristic of signals due to the organic fragments (Silva and Prather, 2000), while lower fraction of the organic fragments at  $m/z$   $77[\text{C}_6\text{H}_5]^+$  and  $91[\text{C}_7\text{H}_7]^+$  were also observed in the mass spectra. The peak series at  $m/z$  51, 63, 77 and 91 are indicative of aromatic signature (Dall’Osto and Harrison, 2012; Silva and Prather, 2000). In addition, peaks corresponding to sodium ( $23[\text{Na}]^+$ ), calcium ( $40[\text{Ca}]^+$ ), and vanadium ( $51[\text{V}]^+/67[\text{VO}]^+$ ) in the positive mass spectra, and  $-26[\text{CN}]^-$  and  $-42[\text{CNO}]^-$  in the negative mass spectra were also detected. The complex mixture of these particles could be attributed to different sources and/or the extensive processing of carbon-containing particles in the atmosphere.

### 3.1 Single-particle classes of carbon-containing particles

Average positive and negative mass spectra for the carbon-containing particle classes for the spring period are presented in Fig. 3, while the results for the fall period were similar, as shown in Fig. S2. A brief description of the mass spectral characteristics of these particle classes was provided as follows.

The mass spectra of Biomass particles presented potassium ( $39[\text{K}]^+$ ) as the highest peaks, combined with carbonaceous ion peaks (generated from both OC and EC), and also K cluster ions with  $\text{Cl}^-$  ( $113[\text{K}_2^{35}\text{Cl}]^+/115[\text{K}_2^{37}\text{Cl}]^+$ ) and with  $\text{SO}_4^{2-}$  ( $213[\text{K}_3^{32}\text{SO}_4]^+/215[\text{K}_3^{34}\text{SO}_4]^+$ ) in relatively low intensity, indicating the biomass origin nature of these particles (Liu et al., 2003; Pratt et al., 2011). The negative ion markers, at  $m/z$   $-45$ ,  $-59$ , and  $-73$  due to levoglucosan, for biomass-burning particles were also detected in these parti-

**Table 1.** Summary of number count and fraction of single-particle classes during spring and fall sampling periods.

Single particle classes	Number count		Number fraction <sup>1</sup>		Scaled number fraction
	Spring	Fall	Spring	Fall	Spring
Biomass	164 590	436 921	23.6 %	61.0 %	13.7 %
OC	69 551	82 508	10.0 %	11.5 %	10.7 %
ECOC	181 885	21 842	26.1 %	3.0 %	4.8 %
EC-fresh	32 279	6961	4.6 %	1.0 %	13.6 %
EC-Sulfate	60 230	81 226	8.6 %	11.4 %	41.5 %
V-ECOC	12 905	885	1.9 %	0.1 %	0.8 %
Amine	23 671	– <sup>2</sup>	3.4 %	–	0.6 %
Others	151 354	85 822	21.8 %	12.0 %	14.3 %
Sea salt	30 213	8812	4.3 %	1.2 %	
Dust-Ca	26 298	–	3.8 %	–	
Dust-Fe	20 551	2273	3.0 %	0.3 %	
Phosphate	1716	3524	0.3 %	0.5 %	
Silicate	–	2349	–	0.3 %	

<sup>1</sup> Number fraction was calculated through dividing the number count of single-particle classes by the total particle count.

<sup>2</sup> The particle class was not identified during this period.

cles although they were in low intensity (Bi et al., 2011). Additionally, peaks corresponding to sulfate and nitrate were commonly observed in the negative mass spectrum, which means that Biomass particles were subjected to atmospheric ageing and acquired a large amount of sulfate and nitrate during transport (Pratt et al., 2011).

ECOC particles were characterized by dominant EC cluster ions, intense OC signals (e.g.,  $m/z$  27, 37, 39 and 43) in the positive mass spectrum, and nitrate and sulfate in the negative mass spectrum. Median peaks at  $m/z$  51 and 63 attributed to aromatic compounds were also observed. There was another ECOC particle type: V-ECOC, which provides a very unique mass spectrum due to strong ion peaks from  $51[\text{V}]^+/67[\text{VO}]^+$ . Vanadium-containing particles have been detected in ambient aerosols (Tolocka et al., 2004; Moffet et al., 2008), and are attributed to residual fuel oil combustion associated with sources such as ships and refineries (Moldanová et al., 2009; Ault et al., 2010), and in a smaller proportion also to vehicles exhaust (Sodeman et al., 2005; Shields et al., 2007).

EC-fresh particles were dominated by dual polarity EC cluster ions with really low intensity of secondary species. It is noted that EC-fresh particles were actually not pure EC but dominated by EC composition since EC-fresh particles usually consisted of weak ion peaks from OC and sulfate. The strongest signals for  $23[\text{Na}]^+$  and  $40[\text{Ca}]^+$  were observed in this particle type. Ca-containing EC particles have previously been detected in the exhaust of automobiles from combusted lubricating oil (Dall’Osto et al., 2009; Spencer et al., 2006), despite the fact that the strong intensity of K may still indicate the biomass/biofuel origin of this particle type. Therefore, this particle type should represent a mixture

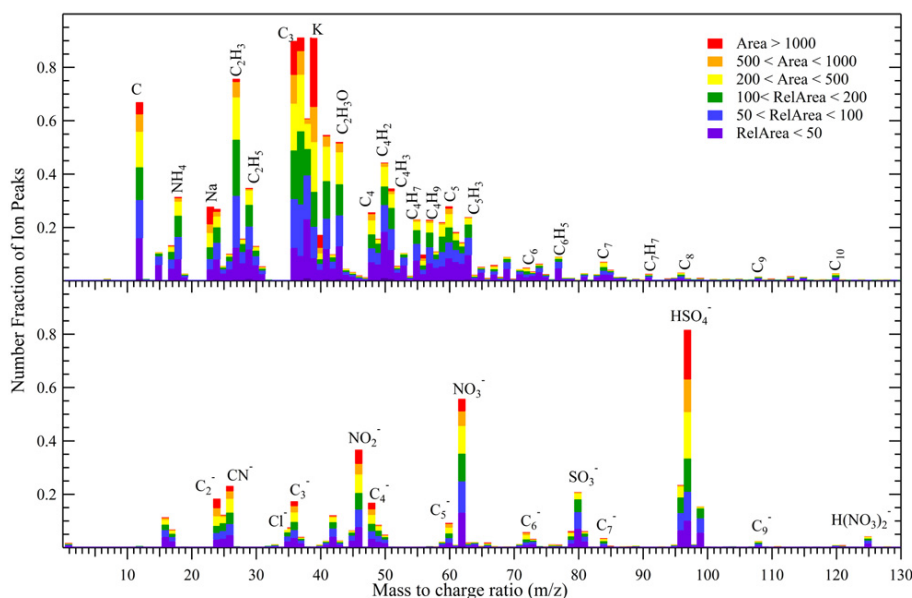


**Fig. 2.** Average digitized positive (upper) and negative (bottom) ions mass spectrum of carbon-containing particles analyzed over the spring period, while that for the fall period was generally similar.

of fresh EC particles from these two combustion processes. Similar to the EC-fresh, EC-Sulfate particles also comprised of peaks from strong EC cluster ions. However, their mass spectra were with strong sulfate signature, and weak signals from nitrate. While  $m/z$   $-97$  might also be assigned to phosphate  $[\text{H}_2\text{PO}_4]^-$  for particles from fresh vehicle exhaust (Toner et al., 2006), the weak existence of fragments at  $m/z$   $-79$   $[\text{PO}_3]^-$  suggests the correct assignment of  $m/z$   $-97$  to  $[\text{HSO}_4]^-$ . These particles were also observed in urbanized Mexico City, and they were suggested to be produced by an oxidation of sulfur in the fuel and rapid condensation onto the existing EC particles in the plume (Moffet and Prather, 2009).

There were two classes of OC dominant particles: OC and Amine. Unlike ECOC particles, mass spectra of OC particles were dominated by intense OC signals (e.g.,  $m/z$  27, 37, 39 and 43). The intense peak corresponding to sulfate was also observed in these particles. Amine particles showed distinct ion peak at  $m/z$   $+59$   $[\text{N}(\text{CH}_3)_3]^+$ , which was assigned to trimethylamine (Angelino et al., 2001; Rehbein et al., 2011). This particle type was exclusively observed during the spring period and significantly enhanced through fog processing as previously reported by our group and the others (Zhang et al., 2012; Rehbein et al., 2011). The relatively less humid air condition (RH 54 %) during the fall period was probably responsible for the missing of Amine particles, since the aerosol water essentially seemed to be the dominant factor to control the gas-to-particle conversion of trimethylamine (Rehbein et al., 2011).

### 3.2 Seasonal variations of carbon-containing particles

Table 1 lists the number fraction of carbon-containing classes calculated based on the unscaled particle number count, with the scaled result during the spring period. Although the unscaled number fractions only provided indicative results instead of quantitative ones, the differences can still be seen between spring and fall. During the spring period, the top three carbon-containing particle classes were ECOC (26.1 %), Biomass (23.6 %) and OC (10 %), respectively. EC-Sulfate (8.6 %) showed a moderate contribution, and the last three classes were EC-fresh (4.6 %), Amine (3.4 %) and V-ECOC (1.9 %). During the fall period, the fraction of Biomass particles increased considerably and became predominant (61.0 %); however, the fraction of V-ECOC (0.1 %) and ECOC (3.0 %) significantly decreased, and Amine particles were nearly absent during this period.

Considerable increase of Biomass particles suggests the significant influence from regional biomass-burning activities on the ambient air quality of urban Guangzhou during the fall period. A fire-dot map (Fig. S3), obtained from the Moderate Resolution Imaging Spectroradiometer (MODIS) on board the Terra and Aqua satellites over a 10 day period, showed that fire dots in the northeast of Guangzhou were intense during this period, and that air parcels through these areas brought in a large amount of biomass-burning particles. The result is consistent with that derived from other studies during the PRIDE-PRD 2004 campaign, which concluded that inputs from biomass burning to Guangzhou are prevalent during the dry northeast monsoon period (Gnauk et al., 2008; Hagler et al., 2006). Through measurements during the

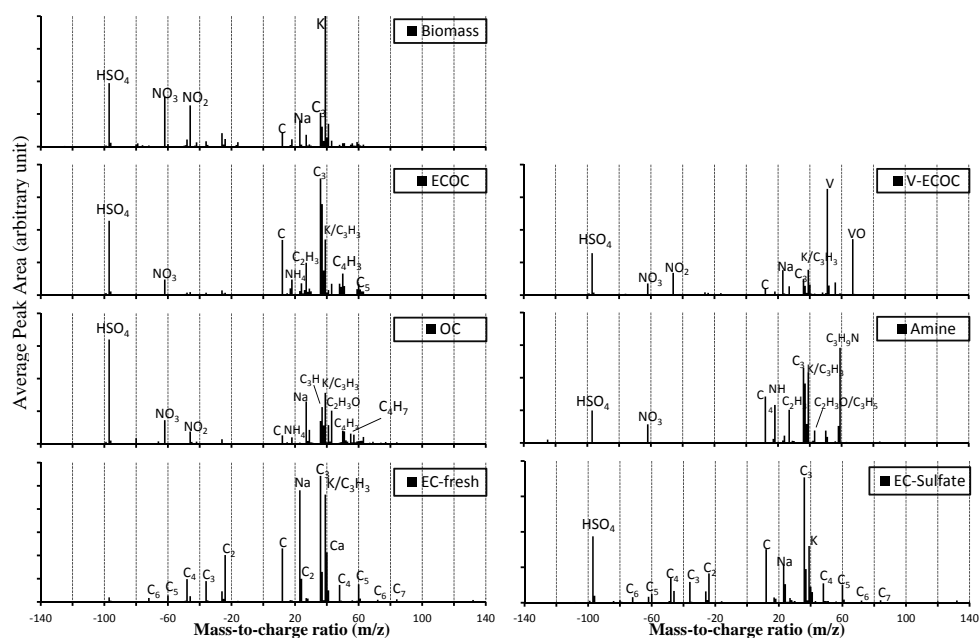


**Fig. 3.** Averaged positive and negative mass spectra for the 7 single-particle classes (Biomass, ECOC, OC, EC-fresh, EC-Sulfate, V-ECOC, and Amine) observed during the whole sampling period in spring.

PRIDE-PRD 2006 campaign, Zhang et al. (2010) also suggested a significant impact of biomass-burning activities in neighboring and/or rural regions on ambient aerosol levels of urban areas in the PRD region, where local sources were limited. Although there were also many fire dots in the neighboring regions during the spring period, the dominant air masses from oceanic areas and the relatively abundant precipitation resulted in minimizing the influence of biomass-burning particles from regional transport. With dissimilarity to Biomass particles, V-ECOC particles were rarely detected during the fall period (0.1 %) compared to those during the spring period (1.9 %), which can be interpreted by the fact that the air masses originated from marine areas were prevalent during the spring period and because ship emissions are suspected to be a dominant source for V-ECOC. Higher fractions of V-ECOC and sea-salt particle classes (Table 1) during the spring period accords with this air-mass history. Considering a more stagnant meteorological condition during the fall should facilitate the formation of SOA (secondary organic aerosol) on particle cores like EC (Tan et al., 2009), the significant decrease in number fraction of ECOC was unexpected and the reason behind this was unclear. With regard to a discussion in the next section, the difference was likely the size distribution of EC-Sulfate between spring and fall seasons.

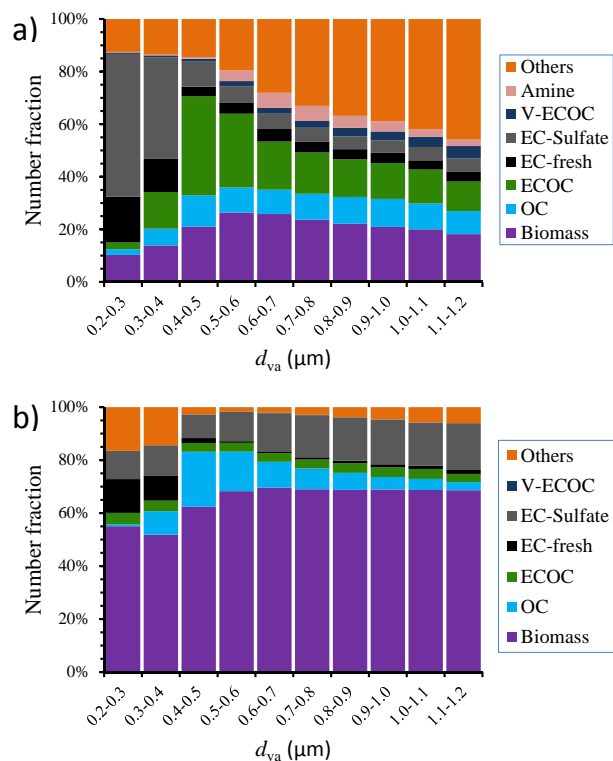
### 3.2.1 Chemically resolved size distribution

Figure 4 shows the size-resolved number fraction of single-particle classes, which was highly variable with  $d_{va}$ . For ex-

ample, during the spring period, EC-fresh and EC-Sulfate particles dominated in the size range of 0.2–0.3  $\mu\text{m}$ , together accounting for 72 % in this size range, while less than 13 % in the size range of 0.4–1.2  $\mu\text{m}$ . The most abundant of EC-Sulfate in the smaller particles might indicate a predominant role of sulfuric acid in the processing of EC (Khalizov et al., 2009). A dominant number fraction of EC was found from the fresh vehicle exhausts in the submicron range (Shields et al., 2007) and ultrafine size ranges ( $< 0.2 \mu\text{m}$ ) (Sodeman et al., 2005). OC and ECOC classes were of minor fraction (less than 3 %) in the size range of 0.2–0.3  $\mu\text{m}$ , implying that EC and OC were more externally mixed in the smaller particles.

The chemical pattern during spring period changed substantially from the smaller (0.2–0.4  $\mu\text{m}$ ) to the larger particles (0.4–1.2  $\mu\text{m}$ ) (Fig. 4a). The number fractions of EC-fresh and EC-Sulfate presented a similar pattern as a function of  $d_{va}$ . They decreased dramatically, while the OC and ECOC classes increased considerably from the smaller to the larger particles. Increased ECOC in the larger particles might be caused by ageing of EC-fresh and EC-Sulfate in the smaller particles through the condensation of semi-volatile species (e.g., ammonium, nitrate and organics) and/or hygroscopic growth, when considering the internal mixing with sulfuric acid dominating the initial ageing processes (Khalizov et al., 2009). Once emitted into the air, the irregular geometry and complex microstructure of EC may provide the active sites for further ageing (Decesari et al., 2002).

The major differences of size-fraction distributions between spring and fall were the Biomass particles, with the



**Fig. 4.** Size-resolved number fractions of single-particle classes for the (a) spring and (b) fall periods.

number fraction larger during the fall than the spring, over the whole size range. In addition, a difference was also produced from the mass spectral characteristics of Biomass particles between spring and fall. It is observed that the relative intensity of the secondary species (i.e., ammonium ( $m/z$  18), organics ( $m/z$  43), nitrate ( $m/z$  -62) and sulfate ( $m/z$  -97)) increased from the smaller to the larger Biomass particles during both periods. The increase of these species was much stronger during the fall than the spring, particularly nitrate and sulfate (Fig. S4). This might further support that the emission of Biomass particles were more likely to be from the local and nearby sources during the spring period, while larger contribution of regional and/or long-range transport was expected in the fall period, as discussed above. Aerosols from regional or long-range transport should experience sufficient ageing processes, typically via addition of secondary species like sulfate and nitrate (Johnson et al., 2005; Roldin et al., 2011), which lead to the growth of particles. Additionally, the number fraction of EC-Sulfate generally increased in the size range of 0.3–1.2  $\mu\text{m}$  with  $d_{va}$  during the fall period (Fig. 4b), which did not happen during the spring period. These particles also contained a much greater and intense  $\text{K}^+$  peak during the fall than the spring, and their temporal trend also highly correlated to that of Biomass particles ( $r = 0.75$ ,  $p < 0.001$ ). The results indicate considerable contribution of the biomass burning to EC-Sulfate particles from regional

and/or long-range transport, which would lead to larger EC-Sulfate particles during the fall period.

The different size distribution pattern of EC-Sulfate particles may contribute to the difference between number fractions of ECOC. It is obvious that the number fraction of EC-Sulfate particles in the size range of 0.2–0.4  $\mu\text{m}$  was higher in the spring. Generally, the smaller-particle number concentration was much higher than the larger particles as measured by SMPS + C. Thus a large number of EC-Sulfate particles in the smaller particles would provide sufficient EC cores for the ECOC formation, which might lead to an increase in the number fraction of ECOC type in the spring.

### 3.2.2 Mixing state

The mixing state of carbon-containing particle classes with the secondary species was also explored. The presence of secondary species on the various carbon-containing particle classes provides an indication of chemical processes. Markers (i.e.,  $m/z$  18, -62 and -97) were selected to represent secondary inorganic species. The peak at  $m/z$  43, is selected to reflect secondary organic species, which could be formed by oxidation reactions and gas-to-particle conversion of organic species (Moffet and Prather, 2009).

Figure 5 displays the mixing state of secondary markers on the carbon-containing particle classes. The larger amount of ammonium was observed during the fall period, and was attributed to the northeastern air masses from agricultural areas. The enhanced fractions of sulfate and oxidized organics were also found in carbon-containing particles. More radiation during the fall period might be favorable for the production of sulfate and oxidized organics through the photochemical reactions (Xiao et al., 2009), which is uncommon during the rainy spring. Intense biomass-burning activities during the fall period might have also contributed to emission of their precursors. However, the number fraction of nitrate of the carbon-containing particle classes was smaller during the fall period. The decrease of nitrate was probably due to the relatively dry air (Hu et al., 2008) and the reduction of its gaseous precursors mainly emitted from the local traffic and industry (Wang et al., 2008), as a result of an air quality guarantee program during the Asian Games in Guangzhou between 1 November and 20 December 2010, when half of the motor vehicles were off the road and many industrial facilities were shutdown.

### 3.2.3 Variation of particle acidity

Here we adopted the relative acidity ratio ( $R_{ra}$ ), defined by Denkenberger et al. (2007) as a sum of the absolute average-peak-areas of nitrate ( $m/z$  -62) and sulfate ( $m/z$  -97) divided by that of ammonium ( $m/z$  18), to represent the aerosol acidity. Although it does not provide the quantitative information on particle acidity, it might still be indicative. The dependence of  $R_{ra}$  on  $d_{va}$  was presented in Fig. 6

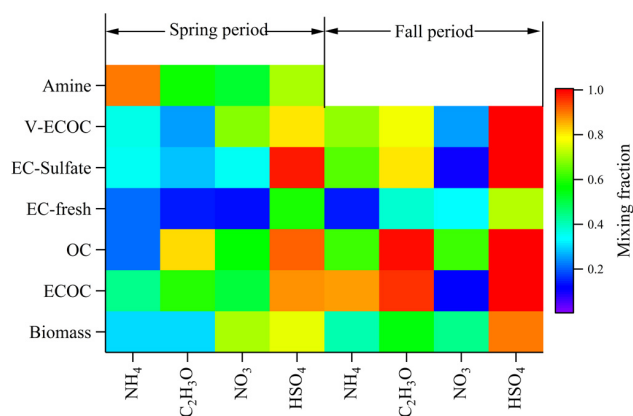


**Fig. 5.** Mixing state of secondary markers with the various carbon-containing particle classes. The color dots represent the number fraction of particle classes (y-axis) that contained the secondary markers (x-axis).

for the spring and fall periods, respectively. In general,  $R_{ra}$  decreased from the smaller to larger particles for the carbon-containing particle classes.  $R_{ra}$  were larger during the spring, consistent with the higher fraction of ammonium causing low acidity of the particles in the fall. The higher relative acidity ratio of EC-fresh in the smaller particles suggested a rapid condensation of sulfuric acid onto the EC surface. Although with low intensity, more than 50 % of EC-fresh particles were found to contain the sulfate signals. It is worthy to note that the EC-Sulfate particles contained a low fraction of ammonium (35 %) and nitrate (35 %), compared to sulfate (97 %), as shown in Fig. 5. This implies that a certain fraction of sulfate might exist in the form of sulfuric acid rather than ammonium bisulfate and/or ammonium sulfate salts, despite of low efficiency of ammonium due to a laser ionization (Gross et al., 2000).

### 3.3 Case study of carbon-containing particles under specific meteorological conditions

Carbon-containing particles during typical periods in the spring and fall were further investigated to highlight the influence of meteorological conditions. Figure 7 shows the hourly scaled number concentration of single-particle classes in the size range of 0.2–0.95  $\mu\text{m}$  during 19–22 May 2010 of the spring period, when typical weather conditions (i.e., rain, fog and cloudy as marked) were observed. Rain generally reduced the particle number concentration through wet deposition. A significant scavenging of particles was obtained during a heavy rain as marked at midday on 21 May, with the number concentration decreasing from  $\sim 1.7 \times 10^4$  to  $\sim 0.5 \times 10^4 \text{ cm}^{-3}$ . During the foggy episode, the particle number concentration increased predominantly as a result of the relatively stagnant meteorological condition, and also probably the contribution from the growth of smaller particles to fit within the detectable size range of SPAMS.

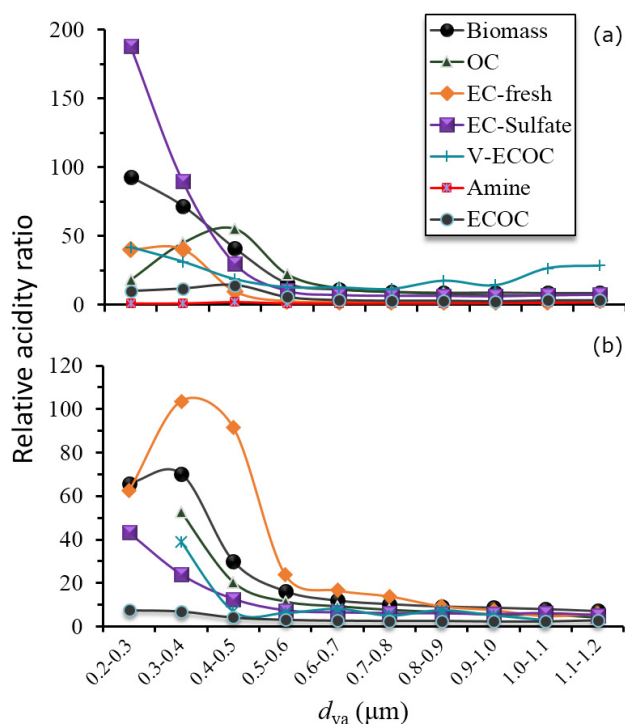


**Fig. 6.** Relative acidity ratio of each single-particle class as a function of  $d_{va}$  for (a) spring and (b) fall periods, respectively.

The foggy episode was identified with the ambient relative humidity exceeding 90 % and the fog processing marker hydroxymethanesulfonate (Munger et al., 1986; Whiteaker and Prather, 2003), the details can be found elsewhere (Zhang et al., 2012).

The fog processing is also expected to influence the chemistry of aerosols. The difference between mass spectra of carbon-containing particle classes before and after the foggy episode is illustrated in Fig. 8. Through the fog processing, OC, ECOC, V-ECOC and EC-Sulfate were generally enhanced with the secondary inorganic species (sulfate, nitrate and/or ammonium). The enhanced secondary inorganic species in aerosols were commonly observed throughout the foggy episodes (Biswas et al., 2008; Safai et al., 2008). However, the EC-fresh and Biomass particles were probably freshly emitted more during the episode, so there was no obvious variation of the secondary species in their mass spectra.

During the fall period, two severe hazy episodes were identified on the 5–6 and 15–17 November 2010, with atmospheric visibility as low as 1.7 and 4 km for Haze 1 and Haze 2, respectively. Similar to that observed during the foggy episodes, the relative intensity of secondary species generally showed an increase from the cloudy to the hazy days (see Fig. 9). The results in this study are consistent with our previous off-line filter measurements conducted in urban

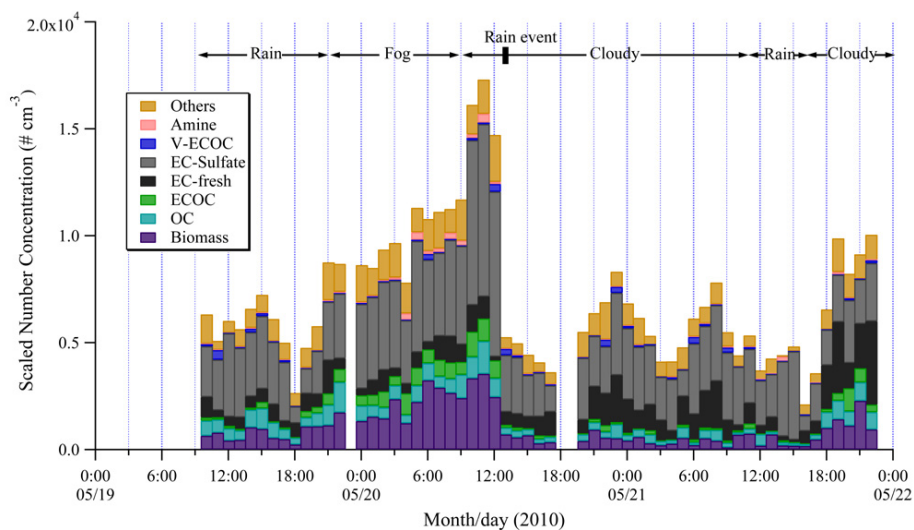


Fig. 7. Temporal profile of the scaled number concentration for each single-particle class during 19–22 May 2010.

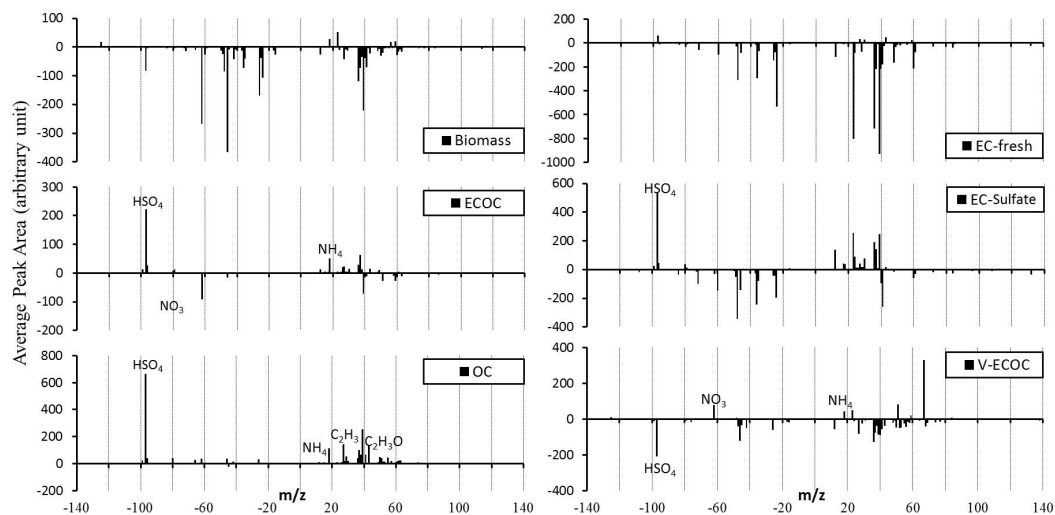


Fig. 8. Difference between mass spectra for carbon-containing particle classes before and after a foggy episode, calculated by subtracting the average peak areas of each single-particle type before the foggy episode from those after the episode.

Guangzhou (Tan et al., 2009), in which the secondary species were found considerably enhanced on the hazy days.

#### 4 Conclusions

In this study, we provide a case study of size-resolved mixing state characteristic of carbon-containing particles in urban Guangzhou during the spring and fall periods of 2010. The carbon-containing particles were the dominant particles in the submicron size range (0.2–1.2  $\mu\text{m}$  in the present study), and were the general characteristic of the distinct single-particle classes (Biomass, OC, ECOC, EC-fresh, EC-Sulfate, V-ECOC and Amine). The spring–fall contrast in prevailing air-mass transport and also meteorological conditions may be

associated with the seasonal variations of chemical pattern, size distribution, mixing state, and aerosol acidity of carbon-containing particles in the urban area of the PRD region.

During the spring period, air masses from the marine region predominated, which impacted the ambient atmosphere in urban Guangzhou with more V-ECOC and sea salt particles. The persistent northeast monsoon during the fall period brought pollutants emitted from the potential source regions in the southeastern China, resulting in significant contribution from the Biomass particles. The relative number fractions of carbon-containing particle classes were strongly variable with  $d_{\text{va}}$ . A high amount of fresh EC particles (i.e., externally mixed) and extensively mixed EC with sulfate were obtained in the size range of 0.2–0.4  $\mu\text{m}$ ,

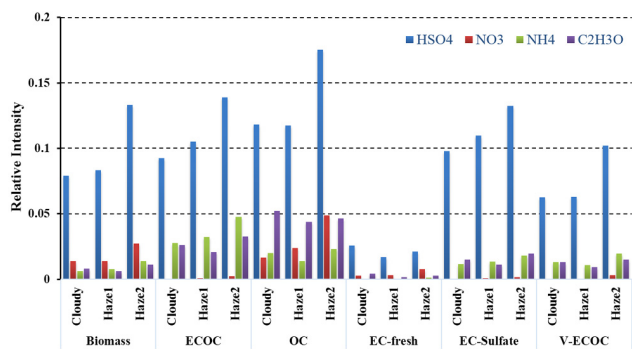


**Fig. 9.** Relative intensities of secondary species on each carbon-containing particle class during cloudy and hazy periods in fall.

particularly during the spring period. The mixing state of carbon-containing particle classes also varied substantially from the spring to fall. Enhanced sulfate and oxidized organics were found in carbon-containing particles during the fall period. Air masses from the northeastern agricultural areas imported a large amount of ammonia into the urban Guangzhou, leading to more frequent appearance and strong intensity of ammonium traces in individual particles during the fall season, which might have an influence on the particle acidity. The case study, under the specific meteorological conditions, also showed that foggy and hazy episodes were involved in the processing of carbon-containing particles, with the addition of secondary species on various particle classes. These results, by direct single-particle observation, provide a reference of mixing state for calculating light extinction, or even modeling the climate forcing of aerosol in the PRD region, with an improvement of validity. They might also help to identify the source and to reveal the atmospheric processes of carbon-containing particles in the PRD region.

**Supplementary material related to this article is available online at:** <http://www.atmos-chem-phys.net/13/4723/2013/acp-13-4723-2013-supplement.pdf>.

**Acknowledgements.** This work was supported by the National Nature Science Foundation of China (No. 41073077), Chinese Academy of Sciences (XDB05010200), and Guangzhou Institute of Geochemistry (GIGCAS 135 project Y234161001). We thank Zhengxu Huang for his assistance during sampling and instrument maintenance. The authors also gratefully acknowledge the NOAA Air Resources Laboratory (ARL) for the provision of the HYSPLIT transport and dispersion model and/or READY website (<http://ready.arl.noaa.gov>) used in this publication. This is contribution no. 1666 from GIGCAS.

Edited by: A. Hofzumahaus

## References

- Andreae, M. O., Schmid, O., Yang, H., Chand, D. L., Yu, J. Z., Zeng, L. M., and Zhang, Y. H.: Optical properties and chemical composition of the atmospheric aerosol in urban Guangzhou, China, *Atmos. Environ.*, 42, 6335–6350, 2008.
- Angelino, S., Suess, D. T., and Prather, K. A.: Formation of aerosol particles from reactions of secondary and tertiary alkylamines: Characterization by aerosol time-of-flight mass spectrometry, *Environ. Sci. Technol.*, 35, 3130–3138, 2001.
- Ault, A. P., Gaston, C. J., Wang, Y., Dominguez, G., Thiemens, M. H., and Prather, K. A.: Characterization of the Single Particle Mixing State of Individual Ship Plume Events Measured at the Port of Los Angeles, *Environ. Sci. Technol.*, 44, 1954–1961, doi:10.1021/es902985h, 2010.
- Bahadur, R., Russell, L., and Prather, K.: Composition and Morphology of Individual Combustion, Biomass Burning, and Secondary Organic Particle Types Obtained Using Urban and Coastal ATOFMS and STXM-NEXAFS Measurements, *Aerosol Sci. Tech.*, 44, 551–562, doi:10.1080/02786821003786048, 2010.
- Bein, K. J., Zhao, Y., Pekney, N. J., Davidson, C. I., Johnston, M. V., and Wexler, A. S.: Identification of sources of atmospheric PM at the Pittsburgh Supersite—Part II: Quantitative comparisons of single particle, particle number, and particle mass measurements, *Atmos. Environ.*, 40, 424–444, doi:10.1016/j.atmosenv.2006.01.064, 2006.
- Bi, X. H., Zhang, G. H., Li, L., Wang, X. M., Li, M., Sheng, G. Y., Fu, J. M., and Zhou, Z.: Mixing state of biomass burning particles by single particle aerosol mass spectrometer in the urban area of PRD, China, *Atmos. Environ.*, 45, 3447–3453, doi:10.1016/j.atmosenv.2011.03.034, 2011.
- Biswas, K. F., Ghauri, B. M., and Husain, L.: Gaseous and aerosol pollutants during fog and clear episodes in South Asian urban atmosphere, *Atmos. Environ.*, 42, 7775–7785, doi:10.1016/j.atmosenv.2008.04.056, 2008.
- Bond, T. C., Doherty, S. J., Fahey, D. W., Forster, P. M., Berntsen, T., DeAngelo, B. J., Flanner, M. G., Ghan, S., Kärcher, B., Koch, D., Kinne, S., Kondo, Y., Quinn, P. K., Sarofim, M. C., Schultz, M. G., Schulz, M., Venkataraman, C., Zhang, H., Zhang, S., Bellouin, N., Guttikunda, S. K., Hopke, P. K., Jacobson, M. Z., Kaiser, J. W., Klimont, Z., Lohmann, U., Schwarz, J. P., Shindell, D., Storelvmo, T., Warren, S. G., and Zender, C. S.: Bounding the role of black carbon in the climate system: A scientific assessment, *J. Geophys. Res.-Atmos.*, doi:10.1002/jgrd.50171, in press, 2013.
- Cahill, J. F., Suski, K., Seinfeld, J. H., Zaveri, R. A., and Prather, K. A.: The mixing state of carbonaceous aerosol particles in northern and southern California measured during CARES and CalNex 2010, *Atmos. Chem. Phys.*, 12, 10989–11002, doi:10.5194/acp-12-10989-2012, 2012.
- Chan, C. K. and Yao, X.: Air pollution in mega cities in China, *Atmos. Environ.*, 42, 1–42, doi:10.1016/j.atmosenv.2007.09.003, 2008.
- Cheng, Y. F., Wiedensohler, A., Eichler, H., Su, H., Gnauk, T., Brüggemann, E., Herrmann, H., Heintzenberg, J., Slanina, J., Tuch, T., Hu, M., and Zhang, Y. H.: Aerosol optical properties and related chemical apportionment at Xinken in Pearl River Delta of China, *Atmos. Environ.*, 42, 6351–6372, 2008.

- Chung, S. H. and Seinfeld, J. H.: Global distribution and climate forcing of carbonaceous aerosols, *J. Geophys. Res.*, 107, 4407, doi:10.1029/2001JD001397, 2002.
- Clarke, A. D., Shinzuka, Y., Kapustin, V. N., Howell, S., Huebert, B., Doherty, S., Anderson, T., Covert, D., Anderson, J., Hua, X., Moore, K. G., McNaughton, C., Carmichael, G., and Weber, R.: Size distributions and mixtures of dust and black carbon aerosol in Asian outflow: Physicochemistry and optical properties, *J. Geophys. Res.-Atmos.*, 109, D15S09, doi:10.1029/2003JD004378, 2004.
- Cubison, M. J., Ervens, B., Feingold, G., Docherty, K. S., Ulbrich, I. M., Shields, L., Prather, K., Hering, S., and Jimenez, J. L.: The influence of chemical composition and mixing state of Los Angeles urban aerosol on CCN number and cloud properties, *Atmos. Chem. Phys.*, 8, 5649–5667, doi:10.5194/acp-8-5649-2008, 2008.
- Dall'Osto, M. and Harrison, R. M.: Urban organic aerosols measured by single particle mass spectrometry in the megacity of London, *Atmos. Chem. Phys.*, 12, 4127–4142, doi:10.5194/acp-12-4127-2012, 2012.
- Dall'Osto, M., Harrison, R. M., Coe, H., and Williams, P.: Real-time secondary aerosol formation during a fog event in London, *Atmos. Chem. Phys.*, 9, 2459–2469, doi:10.5194/acp-9-2459-2009, 2009.
- Decesari, S., Facchini, M. C., Matta, E., Mircea, M., Fuzzi, S., Chughtai, A. R., and Smith, D. M.: Water soluble organic compounds formed by oxidation of soot, *Atmos. Environ.*, 36, 1827–1832, doi:10.1016/s1352-2310(02)00141-3, 2002.
- Denkenberger, K. A., Moffet, R. C., Holecek, J. C., Rebotier, T. P., and Prather, K. A.: Real-time, single-particle measurements of oligomers in aged ambient aerosol particles, *Environ. Sci. Technol.*, 41, 5439–5446, doi:10.1021/es070329l, 2007.
- Draxler, R. R. and Rolph, G. D.: HYSPLIT (HYbrid Single-Particle Lagrangian Integrated Trajectory) Model access via NOAA ARL READY Website (<http://ready.arl.noaa.gov/HYSPLIT.php>), NOAA Air Resources Laboratory, MD, Silver Spring, 2012.
- Fu, H., Zhang, M., Li, W., Chen, J., Wang, L., Quan, X., and Wang, W.: Morphology, composition and mixing state of individual carbonaceous aerosol in urban Shanghai, *Atmos. Chem. Phys.*, 12, 693–707, doi:10.5194/acp-12-693-2012, 2012.
- Gnauk, T., Müller, K., van Pinxteren, D., He, L. Y., Niu, Y. W., Hu, M., and Herrmann, H.: Size-segregated particulate chemical composition in Xinken, Pearl River Delta, China: OC/EC and organic compounds, *Atmos. Environ.*, 42, 6296–6309, 2008.
- Gross, D. S., Galli, M. E., Silva, P. J., and Prather, K. A.: Relative sensitivity factors for alkali metal and ammonium cations in single particle aerosol time-of-flight mass spectra, *Anal. Chem.*, 72, 416–422, 2000.
- Gross, D. S., Galli, M. E., Kalberer, M., Prevot, A. S. H., Dommen, J., Alfarra, M. R., Duplissy, J., Gaeggeler, K., Gascho, A., Metzger, A., and Baltensperger, U.: Real-time measurement of oligomeric species in secondary organic aerosol with the aerosol time-of-flight mass spectrometer, *Anal. Chem.*, 78, 2130–2137, doi:10.1021/ac060138l, 2006.
- Hagler, G. S., Bergin, M. H., Salmon, L. G., Yu, J. Z., Wan, E. C. H., Zheng, M., Zeng, L. M., Kiang, C. S., Zhang, Y. H., Lau, A. K. H., and Schauer, J. J.: Source areas and chemical composition of fine particulate matter in the Pearl River Delta region of China, *Atmos. Environ.*, 40, 3802–3815, doi:10.1016/j.atmosenv.2006.02.032, 2006.
- Healy, R. M., Sciare, J., Poulain, L., Kamili, K., Merkel, M., Müller, T., Wiedensohler, A., Eckhardt, S., Stohl, A., Sarda-Estève, R., McGillicuddy, E., O'Connor, I. P., Sodeau, J. R., and Wenger, J. C.: Sources and mixing state of size-resolved elemental carbon particles in a European megacity: Paris, *Atmos. Chem. Phys.*, 12, 1681–1700, doi:10.5194/acp-12-1681-2012, 2012.
- Huang, X. F., Gao, R. S., Schwarz, J. P., He, L. Y., Fahey, D. W., Watts, L. A., McComiskey, A., Cooper, O. R., Sun, T. L., Zeng, L. W., Hu, M., and Zhang, Y. H.: Black carbon measurements in the Pearl River Delta region of China, *J. Geophys. Res.*, 116, D12208, doi:10.1029/2010jd014933, 2011.
- Huang, X. F., Sun, T. L., Zeng, L. W., Yu, G. H., and Luan, S. J.: Black carbon aerosol characterization in a coastal city in South China using a single particle soot photometer, *Atmos. Environ.*, 51, 21–28, doi:10.1016/j.atmosenv.2012.01.056, 2012.
- Jacobson, M. C., Hansson, H. C., Noone, K. J., and Charlson, R. J.: Organic atmospheric aerosols: Review and state of the science, *Rev. Geophys.*, 38, 267–294, 2000.
- Jacobson, M. Z.: Strong radiative heating due to the mixing state of black carbon in atmospheric aerosols, *Nature*, 409, 695–697, 2001.
- Jacobson, M. Z.: Effects of externally-through-internally-mixed soot inclusions within clouds and precipitation on global climate, *J. Phys. Chem. A*, 110, 6860–6873, doi:10.1021/Jp056391r, 2006.
- Johnson, K. S., Zuberi, B., Molina, L. T., Molina, M. J., Iedema, M. J., Cowin, J. P., Gaspar, D. J., Wang, C., and Laskin, A.: Processing of soot in an urban environment: case study from the Mexico City Metropolitan Area, *Atmos. Chem. Phys.*, 5, 3033–3043, doi:10.5194/acp-5-3033-2005, 2005.
- Khalizov, A. F., Zhang, R. Y., Zhang, D., Xue, H. X., Pagels, J., and McMurry, P. H.: Formation of highly hygroscopic soot aerosols upon internal mixing with sulfuric acid vapor, *J. Geophys. Res.-Atmos.*, 114, D05208, doi:10.1029/2008jd010595, 2009.
- Li, L., Huang, Z. X., Dong, J. G., Li, M., Gao, W., Nian, H. Q., Fu, Z., Zhang, G. H., Bi, X. H., Cheng, P., and Zhou, Z.: Real time bipolar time-of-flight mass spectrometer for analyzing single aerosol particles, *Int. J. Mass. Spectrom.*, 303, 118–124, doi:10.1016/j.ijms.2011.01.017, 2011a.
- Li, W. J., Zhang, D. Z., Shao, L. Y., Zhou, S. Z., and Wang, W. X.: Individual particle analysis of aerosols collected under haze and non-haze conditions at a high-elevation mountain site in the North China plain, *Atmos. Chem. Phys.*, 11, 11733–11744, doi:10.5194/acp-11-11733-2011, 2011b.
- Liu, D. Y., Wenzel, R. J., and Prather, K. A.: Aerosol time-of-flight mass spectrometry during the Atlanta Supersite Experiment: 1. Measurements, *J. Geophys. Res.-Atmos.*, 108, 8426, doi:10.1029/2001JD001562, 2003.
- Moffet, R. C. and Prather, K. A.: In-situ measurements of the mixing state and optical properties of soot with implications for radiative forcing estimates, *Proc. Natl. Acad. Sci. USA*, 106, 11872–11877, doi:10.1073/pnas.0900040106, 2009.
- Moffet, R. C., de Foy, B., Molina, L. T., Molina, M. J., and Prather, K. A.: Measurement of ambient aerosols in northern Mexico City by single particle mass spectrometry, *Atmos. Chem. Phys.*, 8, 4499–4516, doi:10.5194/acp-8-4499-2008, 2008.

- Moldanová, J., Fridell, E., Popovicheva, O., Demirdjian, B., Tishkova, V., Faccinetto, A., and Focsa, C.: Characterisation of particulate matter and gaseous emissions from a large ship diesel engine, *Atmos. Environ.*, 43, 2632–2641, doi:10.1016/j.atmosenv.2009.02.008, 2009.
- Munger, J. W., Tiller, C., and Hoffmann, M. R.: Identification of Hydroxymethanesulfonate in Fog Water, *Science*, 231, 247–249, 1986.
- Pöschl, U.: Atmospheric aerosols: Composition, transformation, climate and health effects, *Angew. Chem. Int. Ed.*, 44, 7520–7540, 2005.
- Prather, K. A.: Our current understanding of the impact of aerosols on climate change, *ChemSusChem*, 2, 377–379, doi:10.1002/cssc.200900037, 2009.
- Pratt, K. A. and Prather, K. A.: Mass spectrometry of atmospheric aerosols Recent developments and applications. Part II: On-line mass spectrometry techniques, *Mass Spectrom. Rev.*, 31, 17–48, doi:10.1002/Mas.20330, 2012.
- Pratt, K. A., Murphy, S. M., Subramanian, R., DeMott, P. J., Kok, G. L., Campos, T., Rogers, D. C., Prenni, A. J., Heymsfield, A. J., Seinfeld, J. H., and Prather, K. A.: Flight-based chemical characterization of biomass burning aerosols within two prescribed burn smoke plumes, *Atmos. Chem. Phys.*, 11, 12549–12565, doi:10.5194/acp-11-12549-2011, 2011.
- Qin, X. Y., Pratt, K. A., Shields, L. G., Toner, S. M., and Prather, K. A.: Seasonal comparisons of single-particle chemical mixing state in Riverside, CA, *Atmos. Environ.*, 59, 587–596, doi:10.1016/j.atmosenv.2012.05.032, 2012.
- Ramanathan, V. and Carmichael, G.: Global and regional climate changes due to black carbon, *Nature Geosci.*, 1, 221–227, doi:10.1038/Ngeo156, 2008.
- Rehbein, P. J. G., Jeong, C. H., McGuire, M. L., Yao, X. H., Corbin, J. C., and Evans, G. J.: Cloud and Fog Processing Enhanced Gas-to-Particle Partitioning of Trimethylamine, *Environ. Sci. Technol.*, 45, 4346–4352, doi:10.1021/es1042113, 2011.
- Reinard, M. S., Adou, K., Martini, J. M., and Johnston, M. V.: Source characterization and identification by real-time single particle mass spectrometry, *Atmos. Environ.*, 41, 9397–9409, doi:10.1016/j.atmosenv.2007.09.001, 2007.
- Roldin, P., Swietlicki, E., Massling, A., Kristensson, A., Löndahl, J., Eriksson, A., Pagels, J., and Gustafsson, S.: Aerosol ageing in an urban plume – implication for climate, *Atmos. Chem. Phys.*, 11, 5897–5915, doi:10.5194/acp-11-5897-2011, 2011.
- Safai, P. D., Kewat, S., Pandithurai, G., Praveen, P. S., Ali, K., Tiwari, S., Rao, P. S. P., Budhawant, K. B., Saha, S. K., and Devara, P. C. S.: Aerosol characteristics during winter fog at Agra, North India, *J. Atmos. Chem.*, 61, 101–118, 2008.
- Shields, L. G., Suess, D. T., and Prather, K. A.: Determination of single particle mass spectral signatures from heavy-duty diesel vehicle emissions for PM<sub>2.5</sub> source apportionment, *Atmos. Environ.*, 41, 3841–3852, 2007.
- Silva, P. J. and Prather, K. A.: Interpretation of mass spectra from organic compounds in aerosol time-of-flight mass spectrometry, *Anal. Chem.*, 72, 3553–3562, 2000.
- Sodeman, D. A., Toner, S. M., and Prather, K. A.: Determination of single particle mass spectral signatures from light-duty vehicle emissions, *Environ. Sci. Technol.*, 39, 4569–4580, 2005.
- Song, X. H., Hopke, P. K., Fergenson, D. P., and Prather, K. A.: Classification of single particles analyzed by ATOFMS using an artificial neural network, ART-2A, *Anal. Chem.*, 71, 860–865, 1999.
- Spencer, M. T., Shields, L. G., Sodeman, D. A., Toner, S. M., and Prather, K. A.: Comparison of oil and fuel particle chemical signatures with particle emissions from heavy and light duty vehicles, *Atmos. Environ.*, 40, 5224–5235, 2006.
- Stroud, C. A., Nenes, A., Jimenez, J. L., DeCarlo, P. F., Huffman, J. A., Bruintjes, R., Nemitz, E., Delia, A. E., Toohey, D. W., Guenther, A. B., and Nandi, S.: Cloud activating properties of aerosol observed during CELTIC, *J. Atmos. Sci.*, 64, 441–459, 2007.
- Sun, J. and Ariya, P.: Atmospheric organic and bio-aerosols as cloud condensation nuclei (CCN): A review, *Atmos. Environ.*, 40, 795–820, 2006.
- Svenningsson, B., Rissler, J., Swietlicki, E., Mircea, M., Bilde, M., Facchini, M. C., Decesari, S., Fuzzi, S., Zhou, J., Mønster, J., and Rosenørn, T.: Hygroscopic growth and critical supersaturations for mixed aerosol particles of inorganic and organic compounds of atmospheric relevance, *Atmos. Chem. Phys.*, 6, 1937–1952, doi:10.5194/acp-6-1937-2006, 2006.
- Tan, J. H., Duan, J. C., Chen, D. H., Wang, X. H., Guo, S. J., Bi, X. H., Sheng, G. Y., He, K. B., and Fu, J. M.: Chemical characteristics of haze during summer and winter in Guangzhou, *Atmos. Res.*, 94, 238–245, 2009.
- Tolocka, M. P., Lake, D. A., Johnston, M. V., and Wexler, A. S.: Number concentrations of fine and ultrafine particles containing metals, *Atmos. Environ.*, 38, 3263–3273, doi:10.1016/j.atmosenv.2004.03.010, 2004.
- Toner, S. M., Sodeman, D. A., and Prather, K. A.: Single particle characterization of ultrafine and accumulation mode particles from heavy duty diesel vehicles using aerosol time-of-flight mass spectrometry, *Environ. Sci. Technol.*, 40, 3912–3921, doi:10.1021/es051455x, 2006.
- Toner, S. M., Shields, L. G., Sodeman, D. A., and Prather, K. A.: Using mass spectral source signatures to apportion exhaust particles from gasoline and diesel powered vehicles in a freeway study using UF-ATOFMS, *Atmos. Environ.*, 42, 568–581, 2008.
- Turpin, B. J. and Huntzicker, J. J.: Identification of Secondary Organic Aerosol Episodes and Quantitation of Primary and Secondary Organic Aerosol Concentrations during SCAQS, *Atmos. Environ.*, 29, 3527–3544, 1995.
- Wang, W., Ren, L., Zhang, Y., Chen, J., Liu, H., Bao, L., Fan, S., and Tang, D.: Aircraft measurements of gaseous pollutants and particulate matter over Pearl River Delta in China, *Atmos. Environ.*, 42, 6187–6202, 2008.
- Whiteaker, J. R. and Prather, K. A.: Hydroxymethanesulfonate as a tracer for fog processing of individual aerosol particles, *Atmos. Environ.*, 37, 1033–1043, 2003.
- Xiao, R., Takegawa, N., Kondo, Y., Miyazaki, Y., Miyakawa, T., Hu, M., Shao, M., Zeng, L. M., Hofzumahaus, A., Holland, F., Lu, K., Sugimoto, N., Zhao, Y., and Zhang, Y. H.: Formation of submicron sulfate and organic aerosols in the outflow from the urban region of the Pearl River Delta in China, *Atmos. Environ.*, 43, 3754–3763, 2009.
- Xiao, R., Takegawa, N., Zheng, M., Kondo, Y., Miyazaki, Y., Miyakawa, T., Hu, M., Shao, M., Zeng, L., Gong, Y., Lu, K., Deng, Z., Zhao, Y., and Zhang, Y. H.: Characterization and source apportionment of submicron aerosol with aerosol mass spectrometer during the PRIDE-PRD 2006 campaign, *Atmos. Chem. Phys.*, 11, 6911–6929, doi:10.5194/acp-11-6911-2011,

- 2011.
- Yang, F., Chen, H., Du, J. F., Yang, X., Gao, S., Chen, J. M., and Geng, F. H.: Evolution of the mixing state of fine aerosols during haze events in Shanghai, *Atmos. Res.*, 104, 193–201, doi:10.1016/j.atmosres.2011.10.005, 2012.
- Yu, H., Wu, C., Wu, D., and Yu, J. Z.: Size distributions of elemental carbon and its contribution to light extinction in urban and rural locations in the pearl river delta region, China, *Atmos. Chem. Phys.*, 10, 5107–5119, doi:10.5194/acp-10-5107-2010, 2010.
- Zhang, G. H., Bi, X. H., Chan, L. Y., Li, L., Wang, X. M., Feng, J. L., Sheng, G. Y., Fu, J. M., Li, M., and Zhou, Z.: Enhanced trimethylamine-containing particles during fog events detected by single particle aerosol mass spectrometry in urban Guangzhou, China, *Atmos. Environ.*, 55, 121–126, doi:10.1016/j.atmosenv.2012.03.038, 2012.
- Zhang, Y. H., Hu, M., Zhong, L. J., Wiedensohler, A., Liu, S. C., Andreae, M. O., Wang, W., and Fan, S. J.: Regional Integrated Experiments on Air Quality over Pearl River Delta 2004 (PRIDE-PRD2004): Overview, *Atmos. Environ.*, 42, 6157–6173, 2008.
- Zhang, Z., Engling, G., Lin, C. Y., Chou, C. C. K., Lung, S. C. C., Chang, S. Y., Fan, S. J., Chan, C. Y., and Zhang, Y. H.: Chemical speciation, transport and contribution of biomass burning smoke to ambient aerosol in Guangzhou, a mega city of China, *Atmos. Environ.*, 44, 3187–3195, doi:10.1016/j.atmosenv.2010.05.024, 2010.